

Chapter 5

Disrupting the Oct4 Octamer DNA Element with Pyrrole-Imidazole Polyamide Conjugates

This project was done in collaboration with John Phillips, Daniel Harki, and James Puckett (Dervan group, Caltech).

John Phillips performed quantitative DNase I footprint titration experiments. Daniel Harki synthesized polyamides **6**, **7**, and **9-14**. James Puckett synthesized polyamides **7** and **8**.

Abstract

Oct4 is a member of the POU family of transcription factors that is expressed in the early stages of the developing embryo and whose activity is exquisitely important in the determination of cell fate. In embryonic stem cells, small changes in Oct4 levels mark the boundary between remaining in an undifferentiated state and differentiating into one of the cell layers. The Oct4 octamer binding site, located adjacent to the Sox2 heptamer binding site, has been mapped in the enhancer regions of several developmental genes, including Sox2, Nanog, and Pou5f1, the gene that encodes Oct4. Pyrrole-imidazole polyamides are synthetic ligands that bind the DNA minor groove at subnanomolar concentrations with programmable sequence specificity. A series of hairpin polyamide conjugates was designed to target the Oct4 octamer DNA element, and quantitative RT-PCR was used to assay the mRNA expression levels of Oct4 target genes. In the P19 mouse embryonal carcinoma cell line, polyamide treatment resulted in a decrease in Utf1 mRNA that was comparable to that of Oct4 RNA interference-treated cells. In addition, the Sox2 mRNA level increased two-fold when P19 cells were treated with Oct4-targeted polyamide, suggesting that de-repression had occurred. When the R1 mouse embryonic stem cell line was incubated with polyamide, a decrease in the Utf1 mRNA level and a two-fold increase in the Nanog mRNA level were measured by quantitative RT-PCR assay. These results indicate that polyamide conjugates modulate the expression levels of Oct4-driven genes that control the determination of cell fate.

5.1. Introduction

Embryonic stem (ES) cells are derived from the inner cell mass of the blastocyst, one of the earliest stages of embryonic development.¹ They are characterized by the capacity for symmetrical self-renewal and the potential to differentiate into all three germ layers: ectoderm, endoderm, and mesoderm.^{1,2} Oct4, Sox2, and Nanog are transcription factors that contribute to the pluripotency of ES cells.³ In particular, Oct4 plays a central role in ES self-renewal.⁴⁻⁶ Control of Oct4 expression within a tight range is essential to maintain pluripotency.⁷ A less than two-fold increase results in differentiation into primitive endoderm and mesoderm, while a 50% decrease causes ES cells to revert to trophectoderm.⁷ The Oct4/Sox2 complex is an important target in regenerative medicine as researchers look to reprogram somatic cells by defined factors.⁸⁻¹²

Oct4 (encoded by the Pou5f1 gene) belongs to the POU (Pit, Oct, UNC) family of transcription factors and binds to an octamer DNA sequence 5'-ATGCAAAT-3'.¹³ These DNA-binding proteins contain two structurally independent domains connected by a variable linker of 15 to 56 amino acids in length.¹³ The POU-specific domain is roughly 75 amino acids in length and binds the 5'-end ATGC, while the POU-homeo domain contains approximately 60 amino acids and binds the 3'-end AAAT.¹³ Oct4 is highly expressed in embryonic stem (ES) cells and is downregulated when these cells differentiate.¹⁴

Oct4 octamer binding sites are often found in close proximity to Sox2 heptamer elements.¹⁴ Oct4 and Sox2 can form a ternary complex with DNA (Figure 5.1).¹⁵ The two proteins can also bind as a heterodimer in the absence of DNA.¹⁴ The enhancers of target genes have been mapped in mice, and these regulatory regions contain an Oct4 binding site located near Sox2 binding elements. These genes include Pou5f1 (the gene that encodes Oct4), Sox2, Nanog, Utf1, Fbx15, and Fgf4 (Figure 5.1).¹⁴ These DNA elements are generally found adjacent to one another, but can be separated by 3 bp, as in the Fgf4 enhancer.



	Sox2	Oct4
i) Pou5f1	CTTTGTT---	ATGCATCT
ii) Sox2	CATTGTG---	ATGCATAT
iii) Nanog	CATTGTA---	ATGCAAAA
iv) Utf1	CATTGTT---	ATGCTAGT
v) Fbx15	CATTGTT---	ATGATAAA
vi) Fgf4	CTTTGTTTGG	ATGCTAAT

Figure 5.1. (top) The 2.6 Å X-ray crystal structure of a POU/HMG/DNA ternary complex (PDB accession code 1GT0).¹⁵ The POU domain of Oct1 is shown in green, and the HMG domain of Sox2 is shown in blue. These two transcription factors interact on the FGF4 enhancer. (bottom) The alignment of Sox and Oct elements from mouse target genes known to bind Sox2 and Oct4.¹⁴ Image rendered by John Phillips using Chimera software.

The regulatory elements that control the expression of the *Pou5f1* gene include a proximal enhancer located about 1.2 kb upstream of the transcription start site and a distal enhancer located about 2 kb upstream.¹⁴ The distal enhancer controls ES cell-specific expression of *Pou5f1* and contains a composite oct-sox element such that Oct4 regulates its own expression.¹⁴ The Sox2 regulatory region also contains two enhancers.¹⁶ It has been proposed that the essential function of Sox2 is to stabilize ES cells in a pluripotent state by maintaining the requisite level of Oct4 expression.¹⁷ It has been shown that increasing the level of Sox2 inhibits the endogenous expression of several Oct4-Sox2 target genes.¹⁸

Nanog is an Oct4 target gene that works together with Oct4 and Sox2 to control ES cell pluripotency.¹⁹ The binding sites of Oct4 and Nanog have been globally mapped in the mouse ES cell genome by the ChIP-PET method and were found to exhibit substantial overlap.²⁰ The oct-sox composite element in the Nanog proximal promoter is centered 175 bp upstream of the transcription start site.³ Downregulation of Oct4 and Nanog by RNA interference was shown to induce differentiation in mouse ES cells.

The enhancers of the *Utf1*, *Fbx15*, and *Fgf4* genes also contain Oct4 octamer binding elements. The *Utf1* regulatory element selectively binds the Oct4-Sox2 complex but not those containing other members of the Oct family.²¹ The *Fbx15* enhancer octamer binding element is centered 530 bp upstream of the transcription start site and contains a noncanonical 5'-ATGATAAA-3' sequence.²² In the *Fgf4* enhancer, the Oct4 and Sox2 binding sites are separated by 3 bp.²³ The crystal structure in Figure 5.1 contains the Oct4-Sox2 complex bound on the *Fgf4* enhancer.¹⁵

Pyrrole-imidazole polyamides bind the minor groove of DNA in a sequence-specific manner at subnanomolar concentrations.^{24,25} The empirically derived “pairing rules” allow for shape-selective recognition of DNA sequences.^{24,25} Polyamides designed to target 5'-WTGCWW-3' are shown with their putative binding sites in the enhancers of Oct4 target genes (Figure 5.2). For the *Pou5f1*, *Sox2*, *Nanog*, and *Utf1* genes, the Oct4 and Sox2 binding sites are found directly adjacent to one another, but these elements are separated by

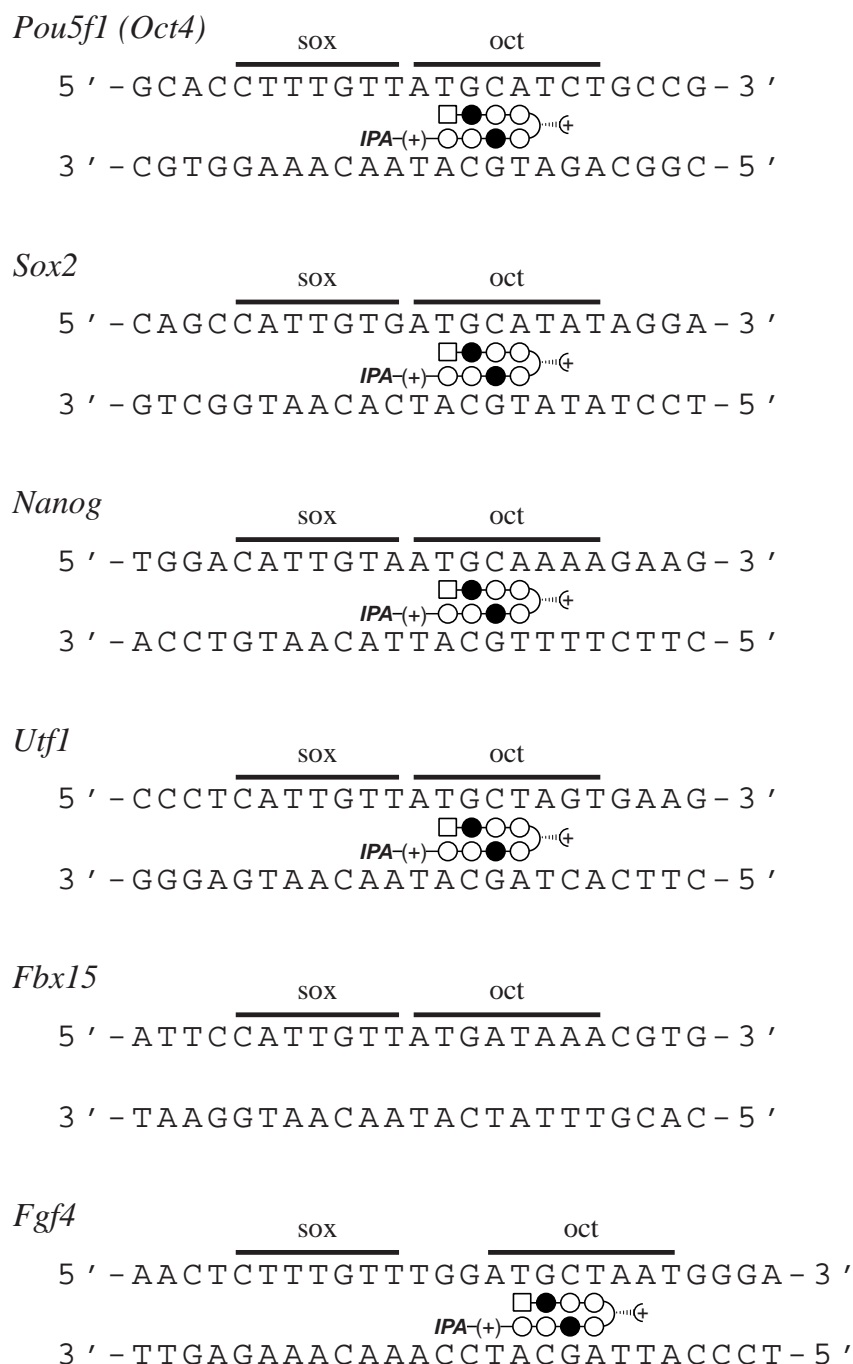


Figure 5.2. Ball-and-stick binding model for the hairpin motif with the polyamide bound to its target DNA sequence within the enhancer regions of Oct4 target genes, including *Pou5f1* (the gene that encodes Oct4), *Sox2*, *Nanog*, *Utf1*, *Fbx15*, and *Fgf4*. Imidazole and pyrrole are shown as filled and non-filled circles, respectively; chlorothiophene is shown as a square; the 3,3'-diamino-*N*-methyldipropylamine linker is shown as "(+)"; and the chiral 3,4-diaminobutyric acid turn residue is shown as a semicircle connecting the two subunits with a dashed wedge linking a half-circle with a plus. The Sox2 heptamer element and the Oct4 octamer element are indicated as "sox" and "oct" above the DNA binding site.

3 bp in the Fgf4 enhancer. The Fbx15 element differs from the 5'-ATGCAAAT-3' octamer sequence by one base pair and would be a mismatch for the designed polyamide.

5.2. Results and discussion

5.2.1. Polyamide design and synthesis

Hairpin pyrrole-imidazole polyamide conjugates are synthetic ligands that bind DNA in a sequence-specific manner with subnanomolar affinity.^{24,25} Polyamides **1-5** were designed to bind the DNA sequence 5'-WTGCWW-3', and their structures are indicated in Figure 5.3. Conjugate **1** contains fluorescein connected to the polyamide with a thiourea linkage to allow direct imaging of cellular uptake by confocal laser scanning microscopy. Conjugates **2-5** contain an isophthalic acid moiety connected to the polyamide with an amide linkage. This class of polyamide conjugates has been shown to exhibit improved nuclear localization.²⁶ Polyamides **2** and **3** contain a chiral 2,4-diaminobutyric acid turn linkage that improves the binding affinity over the achiral variant without loss of sequence specificity.²⁷ Polyamides **4** and **5** contain a chiral 3,4-diaminobutyric acid turn linkage that has been shown to increase the DNA binding affinity further with some, but not all, polyamide cores.²⁸ The acetylated turn linkage used in the design of compounds **1**, **3**, and **5** has been shown to improve nuclear localization in some human cancer cell lines.^{29,30} Polyamides **1-5** were synthesized on oxime resin according to published manual solid-phase synthesis protocols.^{31,32} Fluorescein and isophthalic acid conjugations, as well as the subsequent deprotection and acetylation steps, were performed according to published methods.^{26,28-30} Polyamides **6** and **7** were synthesized as mismatch control compounds for cell culture experiments and have been previously characterized.^{28,33}

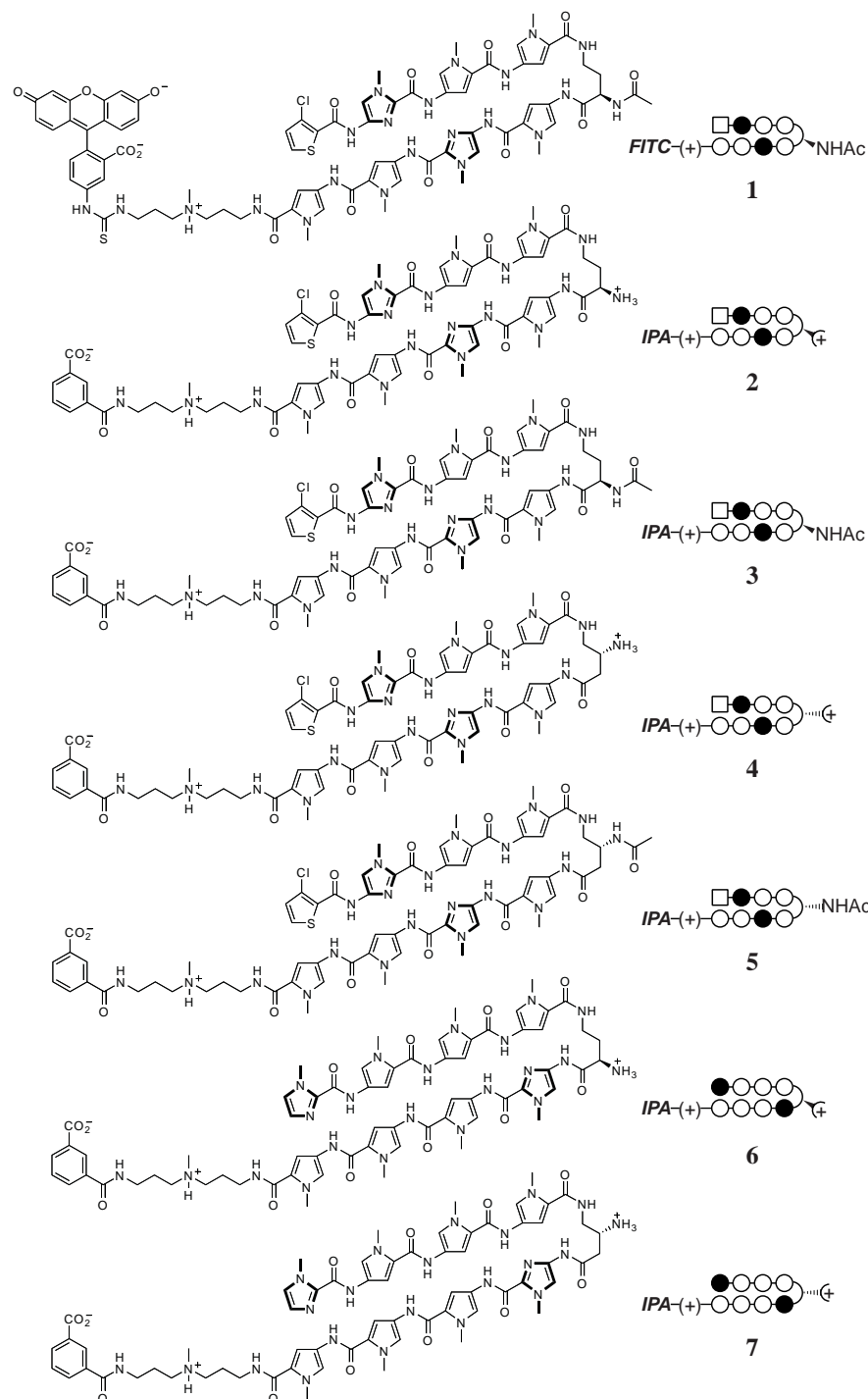


Figure 5.3. Structures of polyamide conjugates 1-7. Imidazole and pyrrole are shown as filled and non-filled circles, respectively; chlorothiophene is shown as a square; the 3,3'-diamino-*N*-methyldipropylamine linker is shown as "(+)"; the chiral 2,4-diaminobutyric acid turn residue is shown as a semicircle connecting the two subunits with a solid wedge linking a half-circle with a plus; and the chiral 3,4-diaminobutyric acid turn residue is shown as a semicircle connecting the two subunits with a dashed wedge linking a half-circle with a plus.

5.2.2. DNase I footprint titrations and melting temperature analysis

The equilibrium association constant (K_a) of polyamide **1** was determined by DNase I footprint titration experiments on the Oct4 binding site of the phOCT4-EGFP1 plasmid obtained from Dr. Wei Cui of the Roslin Institute.³⁴ A partial sequence of this plasmid is shown in Figure 5.18. Polyamide **1** exhibited a binding affinity of $K_a = 8 \times 10^8 \text{ M}^{-1}$ for the DNA sequence 5'-ATGCAT-3' and $K_a = 6 \times 10^8 \text{ M}^{-1}$ for 5'-ATGCTT-3' (Figure 5.4). These experiments indicate that the acetylated polyamide-fluorescein conjugate **1** is a high-affinity DNA binder that exhibits good selectivity, as no other mismatch binding sites were evident in the footprinting gels. As shown in the footprinting data presented in Chapters 4A and 4B, fluorescein conjugation decreases the equilibrium association constant by an order of magnitude.

Melting temperature analysis by UV absorption spectrometry was used to assay the DNA binding affinity of polyamides **1-5**. The 12 bp DNA sequence containing the match site observed in the DNase I footprint titrations was used for this experiment (Figure 5.5). The T_m value for 5'-GAGATGCATGAC-3' and its complement sequence alone was 53.5°C. Polyamide **1** raised the T_m value by 6.0°C, and the reduced steric bulk of the tail moiety in polyamide **3** increased the T_m value by 11.4°C. As expected, the free amine compound **2** exhibited a higher ΔT_m value of 15.5°C. Polyamides containing the 3,4-diaminobutyric acid turn subunit had the highest ΔT_m values. Perhaps surprisingly, acetylated polyamide **5** exhibited a ΔT_m value of 16.7°C that was higher than that of the free amine compound **2**. Polyamide **4** raised the melting temperature by 19.1°C, indicating that its DNA binding affinity was the largest in the series.

5.2.3. Cell culture and confocal microscopy

P19 mouse embryonal carcinoma cells were selected as a model system to measure the expression of Oct4 target genes in cell culture. This cell line was obtained from ATCC and cultured at 37°C in a 5% CO₂ atmosphere according to recommended protocols.

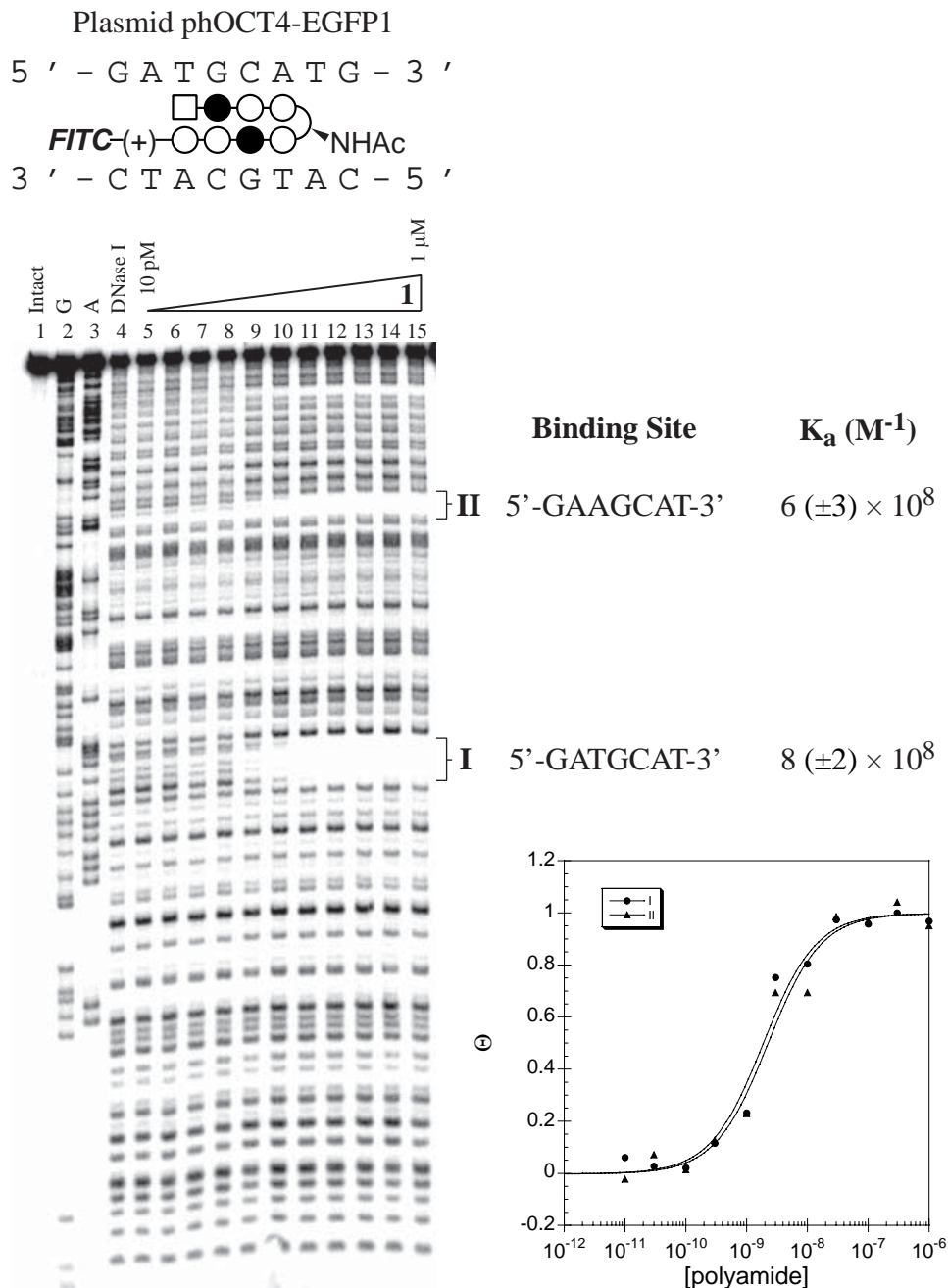


Figure 5.4. Quantitative DNase I footprint titration experiment for polyamide **1** on the 5'-end-labeled PCR product of plasmid phOCT4-EGFP1: lane 1, intact DNA; lane 2, G reaction; lane 3, A reaction; lane 4, DNase I standard; lanes 5-15, 10 pM, 30 pM, 100 pM, 300 pM, 1 nM, 3 nM, 10 nM, 30 nM, 100 nM, 300 nM, 1 μ M polyamide, respectively. Binding isotherms are shown, and θ_{norm} values were calculated according to published methods.³⁷ Imidazole and pyrrole are shown as filled and non-filled circles, respectively; chlorothiophene is shown as a square; the 3,3'-diamino-N-methyldipropylamine linker is shown as “(+)”; and the chiral 2,4-diaminobutyric acid turn residue is shown as a semicircle connecting the two subunits with a solid wedge linking a half-circle with a plus.

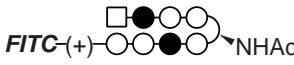
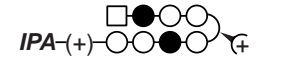
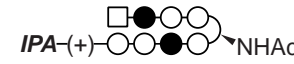
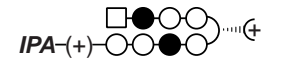
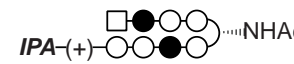
$ \begin{array}{l} 12 \text{ bp DNA} \quad 5' - \text{GAG} \boxed{\text{ATGCA T}} \text{GAC} - 3' \\ \quad \quad \quad 3' - \text{CTC} \boxed{\text{TACGTA}} \text{CTG} - 5' \end{array} $			
	Polyamide	T_m (°C)	ΔT_m (°C)
	DNA only	53.5 (0.3)	
1		59.5 (0.4)	6.0
2		69.0 (0.2)	15.5
3		64.9 (0.2)	11.4
4		72.6 (0.4)	19.1
5		70.2 (0.3)	16.7

Figure 5.5. DNA melting temperature analysis. Experiments were performed with a final concentration of 2 μM of DNA oligonucleotides and polyamides **1-5** in a buffer of 10 mM sodium cacodylate, 10 mM KCl, 10 mM MgCl_2 , and 5 mM CaCl_2 at pH 7.0. Imidazole and pyrrole are shown as filled and non-filled circles, respectively; chlorothiophene is shown as a square; the 3,3'-diamino-*N*-methyldipropylamine linker is shown as “(+)”; the chiral 2,4-diaminobutyric acid turn residue is shown as a semicircle connecting the two subunits with a solid wedge linking a half-circle with a plus; and the chiral 3,4-diaminobutyric acid turn residue is shown as a semicircle connecting the two subunits with a dashed wedge linking a half-circle with a plus. Error values in parentheses indicate standard deviations of quadruplicate experiments.

P19 cells were incubated for 12 h with polyamide **1** to determine the extent of nuclear localization. Direct imaging by confocal laser scanning microscopy was used to image cellular uptake. Polyamide **1** was observed to localize to the nucleus of P19 cells (Figure 5.6). However, the uptake profile in HeLa cells was better than that in P19 cells, suggesting that high polyamide concentrations would be necessary to see changes in gene expression. In Chapter 3, it was observed that a polyamide-fluorescein conjugate showed higher nuclear concentration in U251 cells than in HeLa cells.

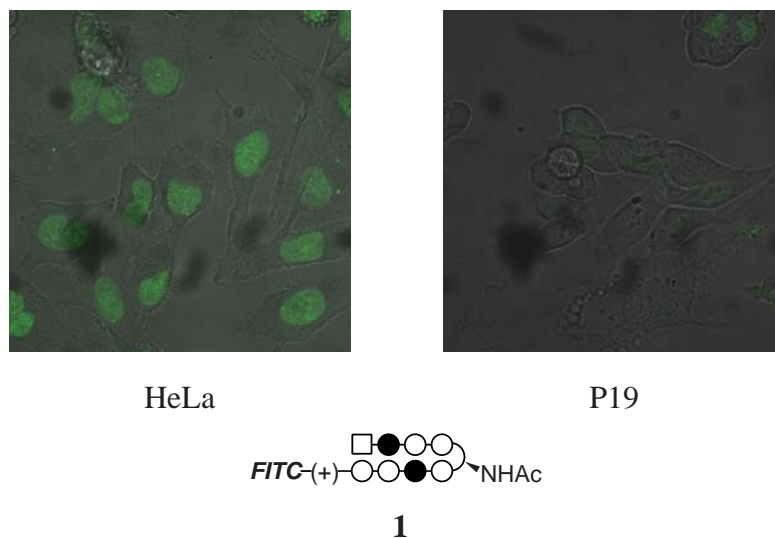


Figure 5.6. Confocal laser scanning microscopy images of polyamide-fluorescein conjugate **1** in HeLa and P19 cell lines. Cells were incubated with 2 μM polyamide for 12 h at 37°C in a 5% CO_2 atmosphere. Imidazole and pyrrole are shown as filled and non-filled circles, respectively; chlorothiophene is shown as a square; the 3,3'-diamino-*N*-methyldipropylamine linker is shown as "(+)"; and the chiral 2,4-diaminobutyric acid turn residue is shown as a semicircle connecting the two subunits with a solid wedge linking a half-circle with a plus.

5.2.4. Quantitative RT-PCR experiments in P19 cells

For cell culture experiments, P19 mouse embryonal carcinoma cells were plated in a 24-well format and incubated with polyamides for 48 h. The time course for this protocol is illustrated in Figure 5.7. At the conclusion of the experiment, RNA was harvested, and quantitative RT-PCR was performed to measure the gene expression levels of Oct4 target genes relative to the housekeeping gene Gapdh. Polyamides **2** and **6** were assayed at 10 μM and 20 μM . Lower concentrations (2.5 μM and 5 μM) did not change gene expression levels. Polyamide **6** was previously shown to bind the prostate-specific antigen (PSA) androgen response element and downregulate androgen-induced PSA genes in cultured prostate cancer cells.³³ Stealth RNAi duplexes from Invitrogen designed to silence the Pou5f1 gene, which encodes Oct4, were used as a positive control. All three duplexes were effective in reducing Pou5f1 gene expression levels greater than 80%, and duplex

Time course for 48-hour experiment (P19 mouse embryonal carcinoma cells)

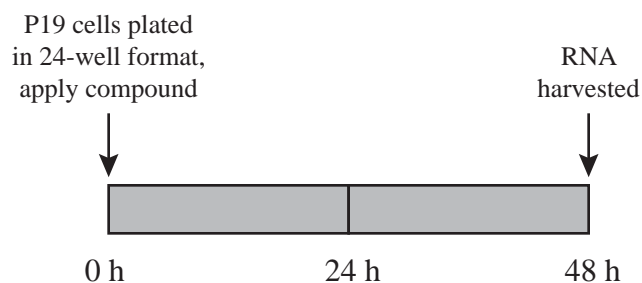


Figure 5.7. Time course for 48-hour incubation experiments with P19 mouse embryonal carcinoma cells. P19 cells were plated in 24-well format at $t = 0$ h, and compounds were applied at this time. RNA was harvested at the conclusion of the experiment ($t = 48$ h).

#2 achieved the greatest knockdown effect. A mismatch Stealth RNAi with medium GC content was used as a negative control.

Oct4 mRNA levels were unchanged by polyamides **2** and **6**, while the RNAi decreased mRNA levels by 90%, as shown in Figure 5.8. Utf1 mRNA levels decreased in the presence of match polyamide **2**, as would be expected by the disruption of Oct4 transcription factor binding at the octamer DNA element in the enhancer region of the Utf1 gene. Sox2 and Nanog mRNA levels increased in a dose-dependent manner in the presence of polyamide **2**. All four target genes assayed displayed a sequence-specific effect, as mismatch polyamide **6** at 10 μ M and 20 μ M concentrations did not change expression levels.

Polyamides **2-5** were assayed at 20 μ M to determine whether compounds with increased ΔT_m values and acetylated turn linkages would show larger changes in gene expression levels (Figure 5.9). Gene expression was largely unchanged in the presence of acetylated compounds **3** and **5**, suggesting that this class of compounds does not exhibit good cellular uptake in P19 cells. On the other hand, Utf1 mRNA levels decreased in the presence of 20 μ M of polyamides **2** and **4**, which contain a free chiral amine on the turn subunit. Sox2 mRNA increased three-fold when P19 cells were incubated with 20 μ M of

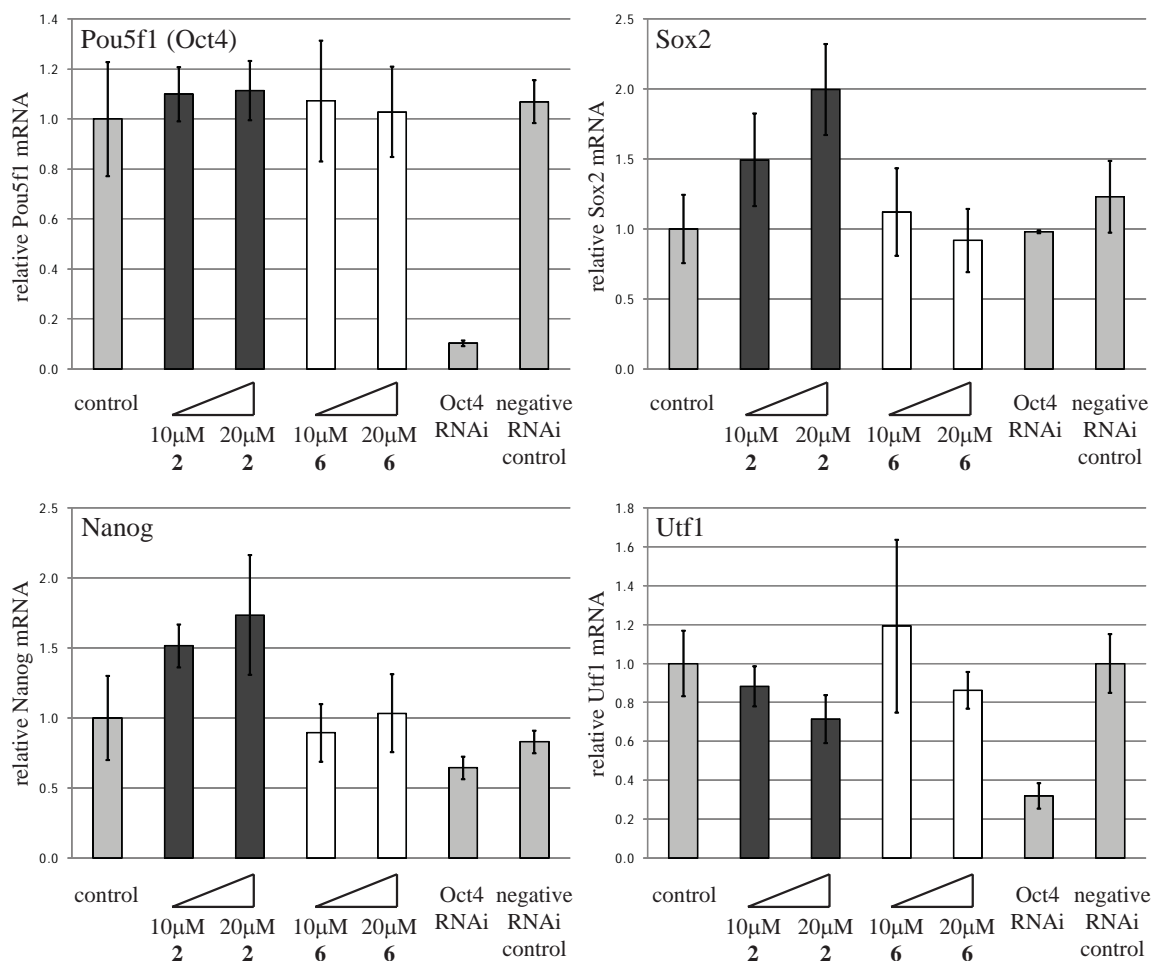


Figure 5.8. Quantitative RT-PCR experiments with polyamides **2** and **6** at 10 μ M and 20 μ M final concentration with 48 h incubation in P19 mouse embryonal carcinoma cells. Stealth RNAi targeted to Pou5f1 (Oct4) and a negative Stealth RNAi control are also shown. The mRNA levels of Pou5f1 (Oct4), Sox2, Nanog, and Utf1 are calculated relative to Gapdh, and error bars indicate standard deviations.

polyamide **4**. However, at these high concentrations of polyamide **4**, some dead P19 cells were evident at the conclusion of the experiment.

Polyamides **4** and **7** were assayed at lower concentrations of 2.5 μ M and 5 μ M to avoid cell toxicity (Figure 5.10). Polyamide **7** was previously shown to inhibit androgen receptor-mediated PSA expression in a prostate cancer cell line.²⁸ Changes in gene expression levels at these concentration ranges were similar to those observed with match polyamide **2** at 10 μ M and 20 μ M. Notably, Utf1 mRNA was decreased to a level comparable to that of the RNAi control, and the Sox2 mRNA level increased two-fold.

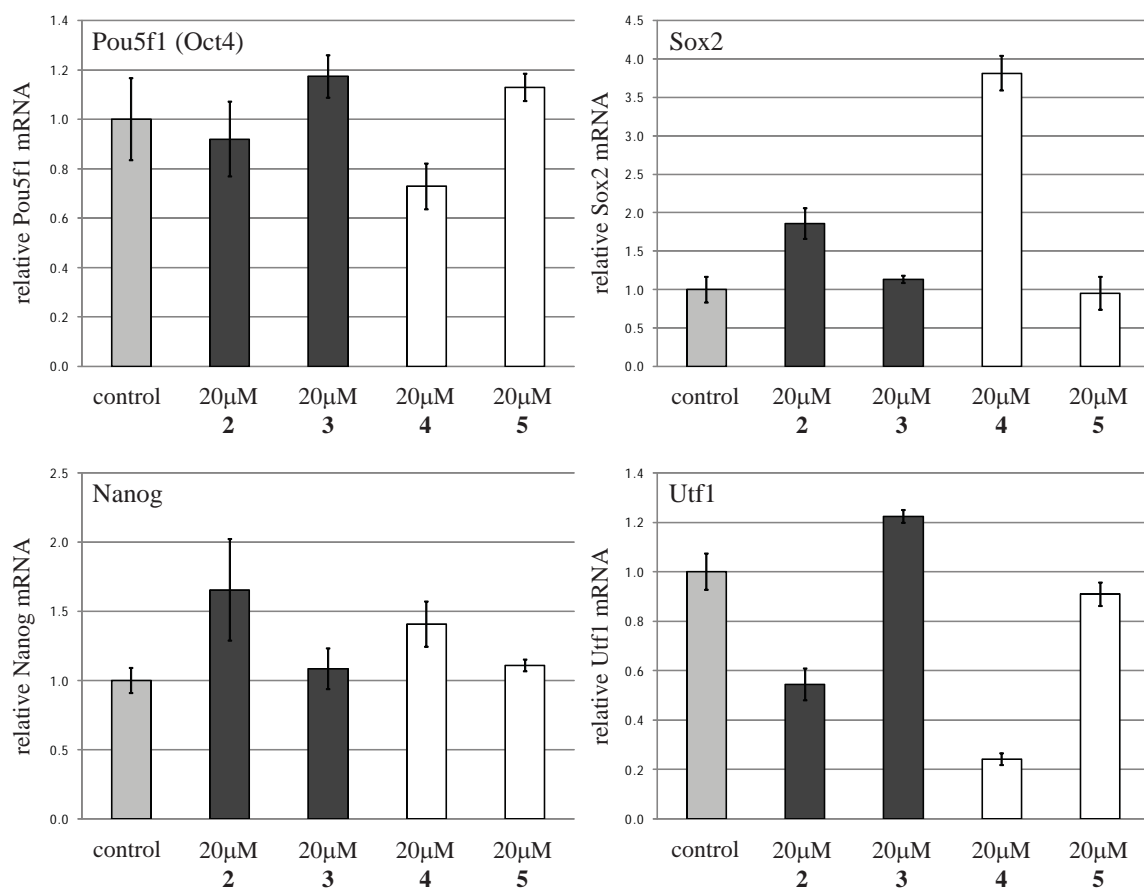


Figure 5.9. Quantitative RT-PCR experiments with polyamides **2-5** at 20 μ M final concentration with 48 h incubation in P19 mouse embryonal carcinoma cells. The mRNA levels of Pou5f1 (Oct4), Sox2, Nanog, and Utf1 are calculated relative to Gapdh, and error bars indicate standard deviations.

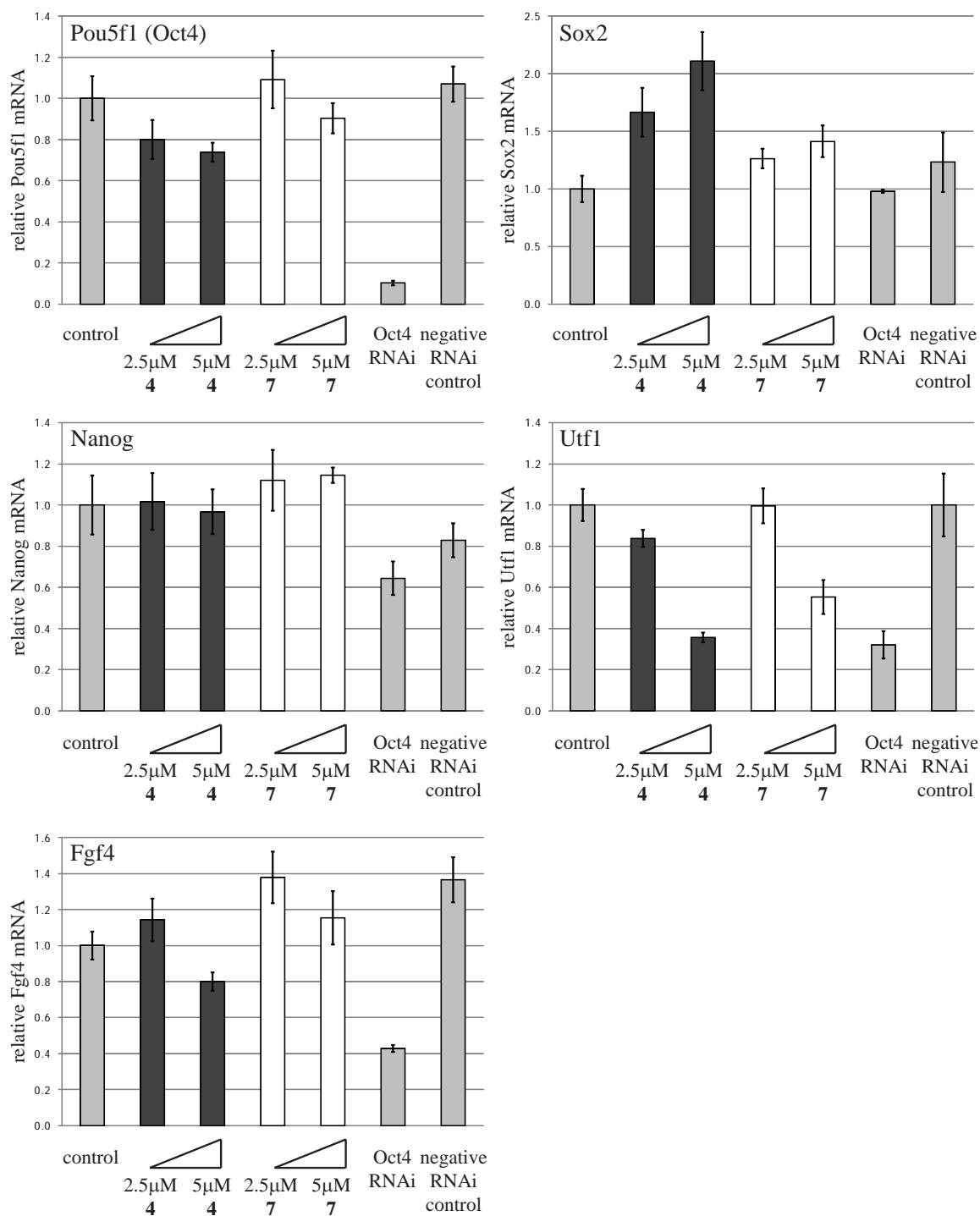


Figure 5.10. Quantitative RT-PCR experiments with polyamides **4** and **7** at 2.5 μ M and 5 μ M final concentration with 48 h incubation in P19 mouse embryonal carcinoma cells. Stealth RNAi targeted to Pou5f1 (Oct4) and a negative Stealth RNAi control are also shown. The mRNA levels of Pou5f1 (Oct4), Sox2, Nanog, Utf1, and Fgf4 are calculated relative to Gapdh, and error bars indicate standard deviations.

5.2.5. Quantitative RT-PCR experiments in R1 mouse ES cells

Based on these results in the model P19 cell line, similar qRT-PCR experiments were performed in R1 mouse embryonic stem (ES) cells. R1 mouse ES cells were maintained according to standard protocols by Caltech Genetically Engineered Mouse Services. In addition to compounds **4** and **7**, two polyamide cocktails were administered (Figure 5.11). Cocktail 1 contained 5 μ M each of polyamides **6**, **8**, **9**, and **10**. Cocktail 2 contained 5 μ M each of polyamides **11-14**. The effects of polyamides **8-10** in cell culture have been previously reported.^{28,33,35} The time course for the 48-hour incubation experiment is illustrated in Figure 5.12. At $t = 0$ h, R1 cells were plated in a 24-well format. After 24 hours, the medium was changed, and compounds were applied. After 48 hours, the medium was changed, and compounds were re-applied. After 72 hours, RNA was harvested.

At the conclusion of the 48-hour incubation, all of the experimental samples appeared morphologically similar to the control untreated cells. Gene expression levels were measured by quantitative RT-PCR (Figure 5.13). *Utf1* mRNA levels decreased in the presence of the match polyamide **4** but showed a similar effect in the presence of mismatch polyamide **7**. *Sox2* and *Nanog* mRNA levels increased in the presence of the tested compounds.

An additional experiment with R1 mouse ES cells was designed to increase the incubation period to 72 hours, allowing more time for potential phenotypic changes.³⁶ Instead of harvesting after 72 hours, the medium was changed and compound was re-applied for a third time (Figure 5.12). RNA was harvested at $t = 96$ hours after plating. Match polyamide **4** was assayed at 5 μ M and 10 μ M concentrations to determine whether higher polyamide concentration and increased incubation time would modulate gene expression further. Retinoic acid has been shown to chemically induce the differentiation of mouse ES cells. A final concentration of 2 μ M retinoic acid was administered to a set of wells in a solution of absolute ethanol. An analogous set of ethanol control wells was prepared for comparison.

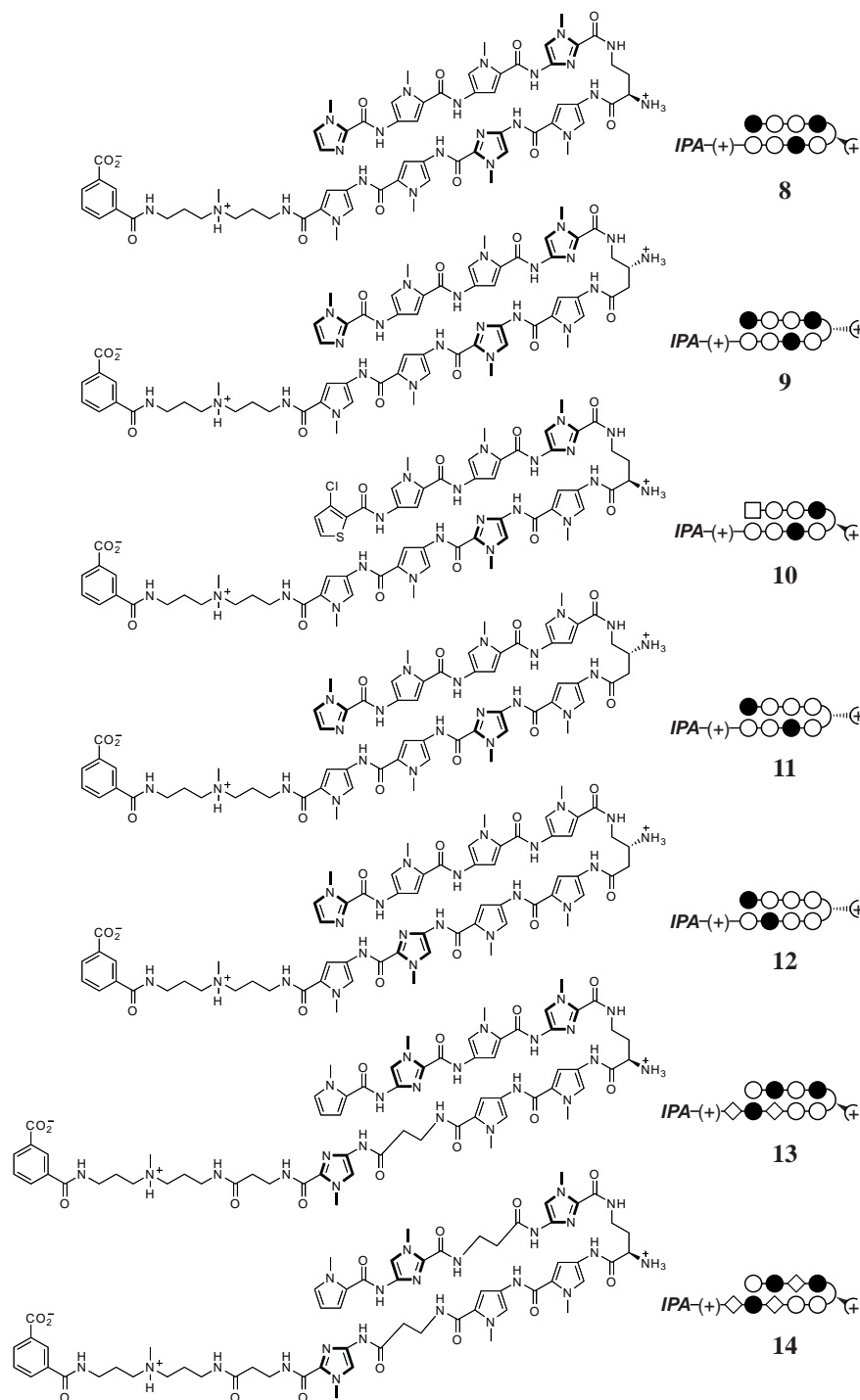
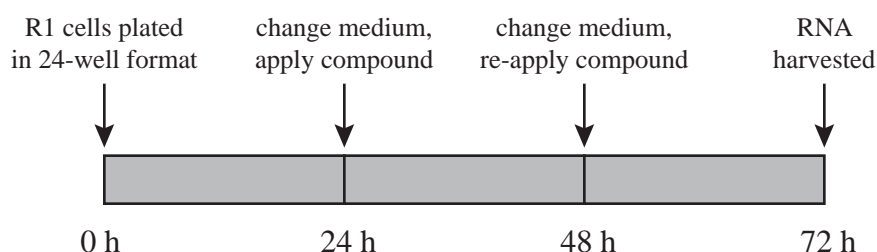


Figure 5.11. Structures of polyamide conjugates **8-14**. Imidazole and pyrrole are shown as filled and non-filled circles, respectively; chlorothiophene is shown as a square; β -alanine is shown as a diamond; the 3,3'-diamino-*N*-methyldipropylamine linker is shown as “(+)”; the chiral 2,4-diaminobutyric acid turn residue is shown as a semicircle connecting the two subunits with a solid wedge linking a half-circle with a plus; the chiral 3,4-diaminobutyric acid turn residue is shown as a semicircle connecting the two subunits with a dashed wedge linking a half-circle with a plus.

Time course for 48-hour experiment (R1 mouse embryonic stem cells)



Time course for 72-hour experiment (R1 mouse embryonic stem cells)

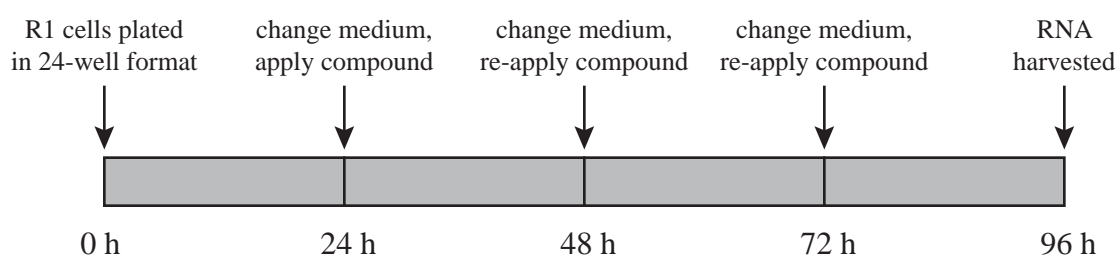


Figure 5.12. Time course for 48-hour and 72-hour incubation experiments with R1 mouse embryonic stem cells. R1 cells were plated in 24-well format at $t = 0$ h, and compounds were first applied at $t = 24$ h. Medium was changed every 24 hours, and compounds were re-applied at this time. RNA was harvested at the conclusion of the experiment ($t = 72$ h for the 48-hour incubation experiment; $t = 96$ h for the 72-hour incubation experiment).

As observed in the previous experiment, Oct4 mRNA levels were unchanged in the presence of match polyamide (Figure 5.14). After 72 hours of incubation with 10 μ M of polyamide **4**, Utf1 mRNA levels decreased over 40%. A comparison of 48-hour and 72-hour incubation periods for 5 μ M of polyamide **4** indicates that a similar level of downregulation was observed at both time points. Nanog mRNA levels increased two-fold after 72 hours of incubation with 10 μ M of polyamide **4**. Based on a comparison of experiments with 5 μ M of polyamide **4**, Nanog mRNA levels were higher after 48 hours of incubation than after 72 hours. Treatment with 2 μ M retinoic acid yielded a 70% decrease in Utf1 mRNA levels and a 2.5-fold increase in Nanog mRNA levels.

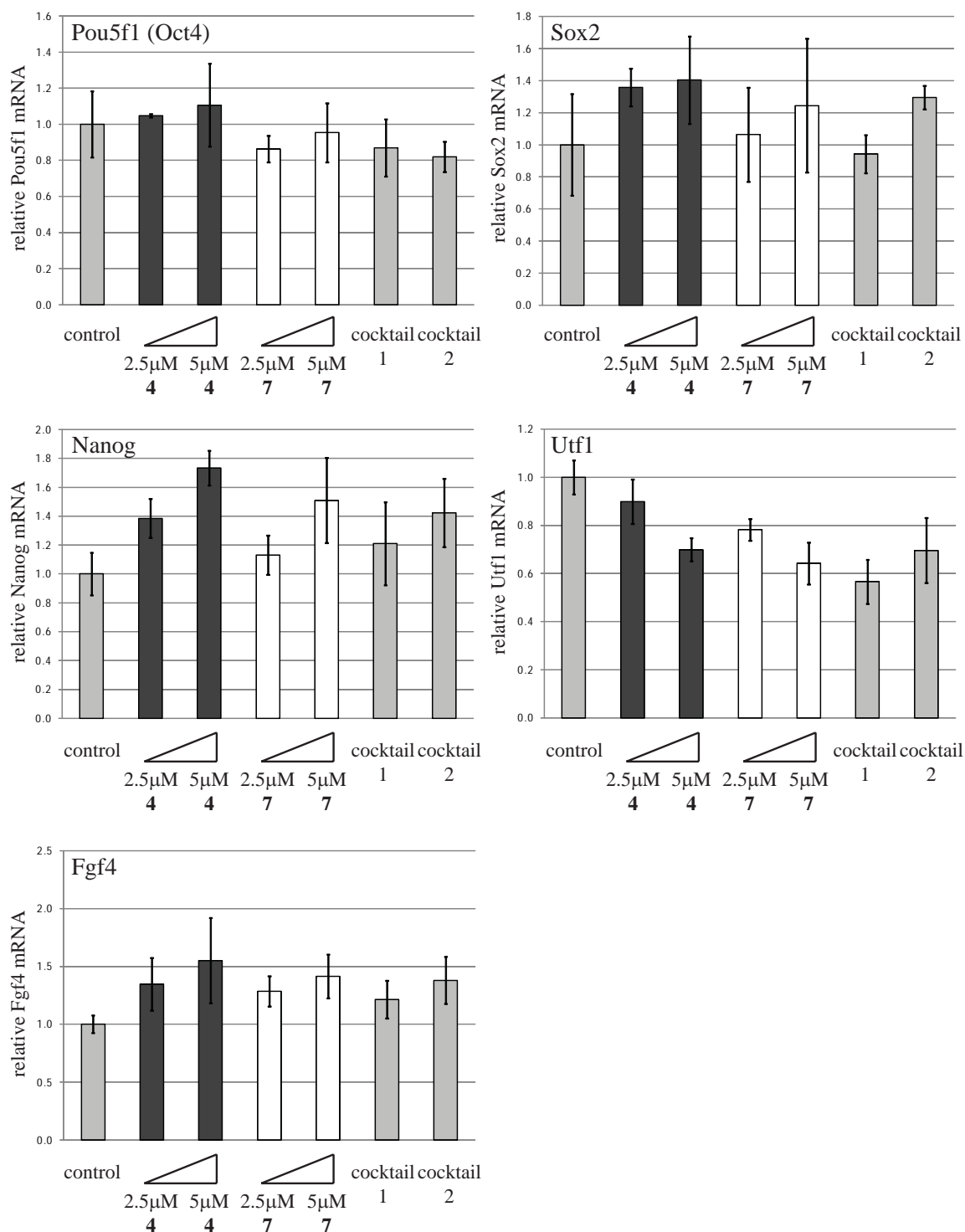


Figure 5.13. Quantitative RT-PCR experiments with polyamides **4** and **7** at 2.5 μ M and 5 μ M final concentration with 48 h incubation in R1 mouse embryonic stem cells. Cocktail 1 contains 5 μ M each of polyamides **6**, **8**, **9**, and **10**. Cocktail 2 contains 5 μ M each of polyamides **11-14**. The mRNA levels of Pou5f1 (Oct4), Sox2, Nanog, Utf1, and Fgf4 are calculated relative to Gapdh, and error bars indicate standard deviations.

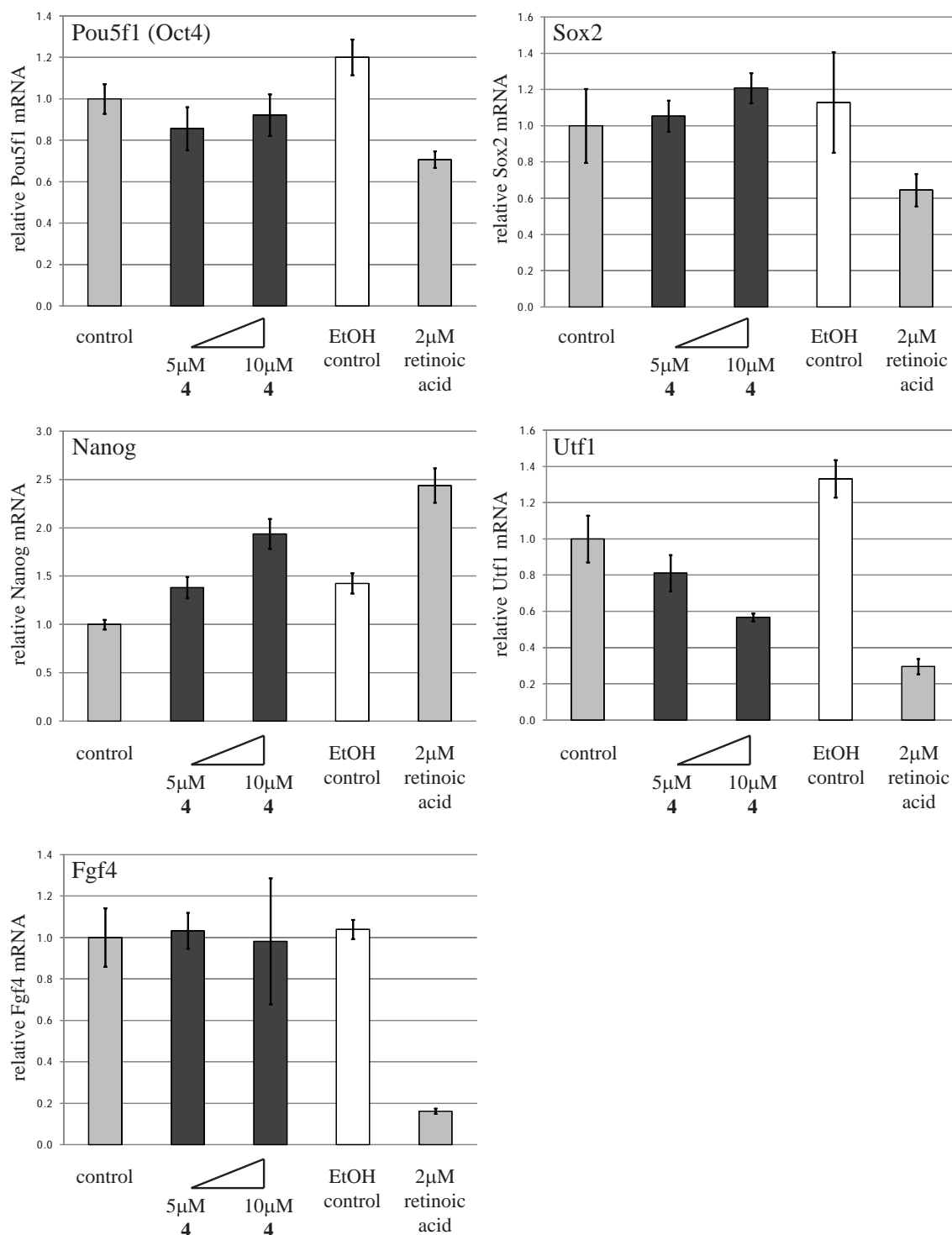


Figure 5.14. Quantitative RT-PCR experiments with polyamide **4** at 5 μ M and 10 μ M final concentration with 72 h incubation in R1 mouse embryonic stem cells. Retinoic acid was added as a solution in ethanol to a final concentration of 2 μ M. The mRNA levels of Pou5f1 (Oct4), Sox2, Nanog, Utf1, and Fgf4 are calculated relative to Gapdh, and error bars indicate standard deviations.

The cell morphology of polyamide-treated and EtOH-treated cells was similar to that of untreated control R1 mouse ES cells. However, the cell morphology of the retinoic acid-treated cells diverged from that of control cells after 24 hours of incubation (Figure 5.15). Retinoic acid-treated cells were healthy after 48 hours and remained divergent in appearance when compared with control cells (Figure 5.16). Based on a picture of these cells at higher magnification, it appeared that these cells were differentiating. After 72 hours of incubation, the polyamide-treated and EtOH-treated cells were healthy and nearly confluent (Figure 5.17). The morphology of these experimental samples was similar to that of the untreated cells. Retinoic acid-treated cells continued to show a different morphology. However, at the conclusion of the 72-hour incubation period, these cells began to look unhealthy, and some colonies had begun to lift off the bottom of the plate.

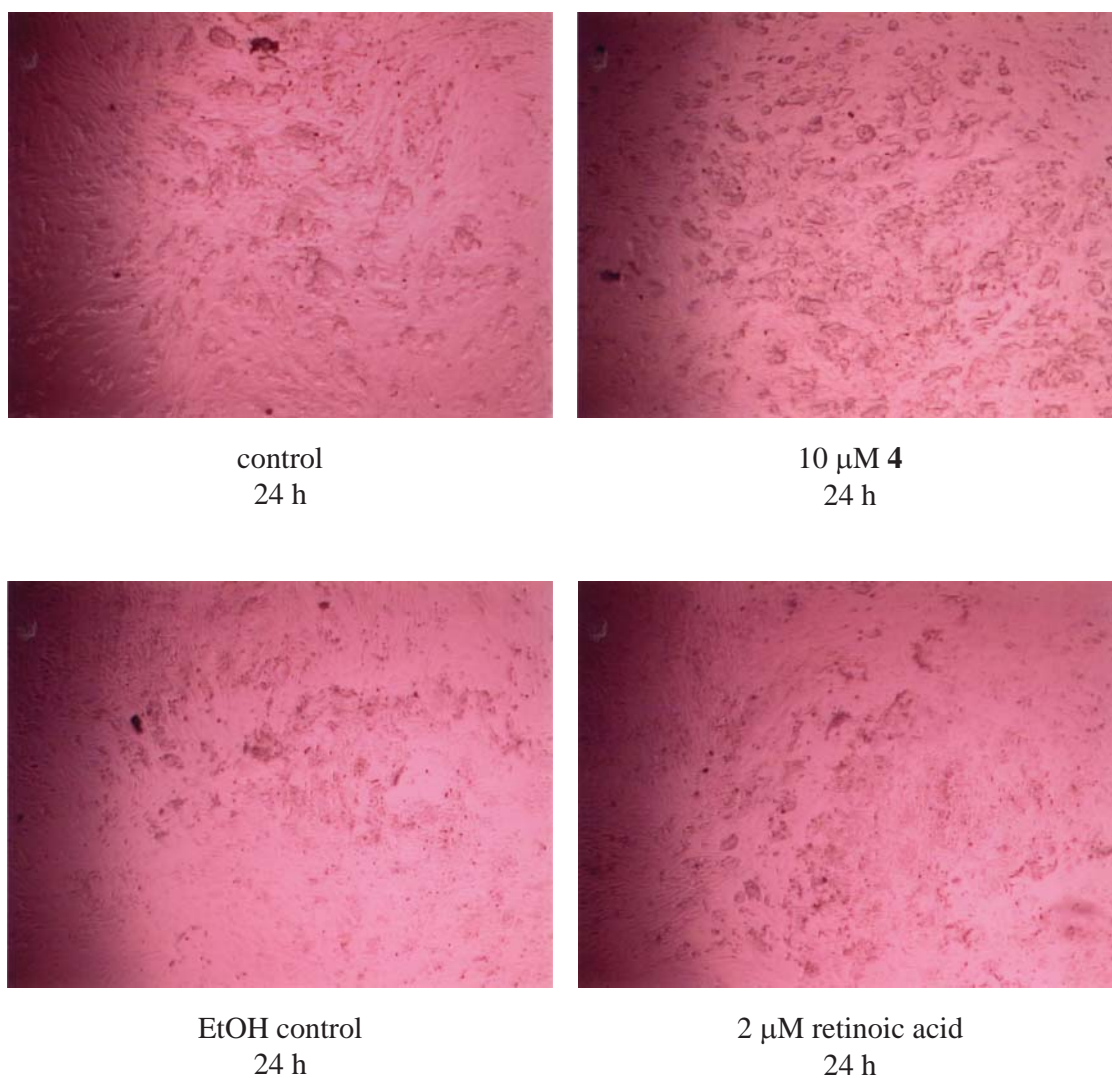


Figure 5.15. Images of R1 mouse embryonic stem cells after 24 h treatment. Untreated cell samples, as well as samples treated with 10 μ M **4**, EtOH only, and 2 μ M retinoic acid dosed in EtOH, are shown following 24 hours of incubation with the compound indicated.

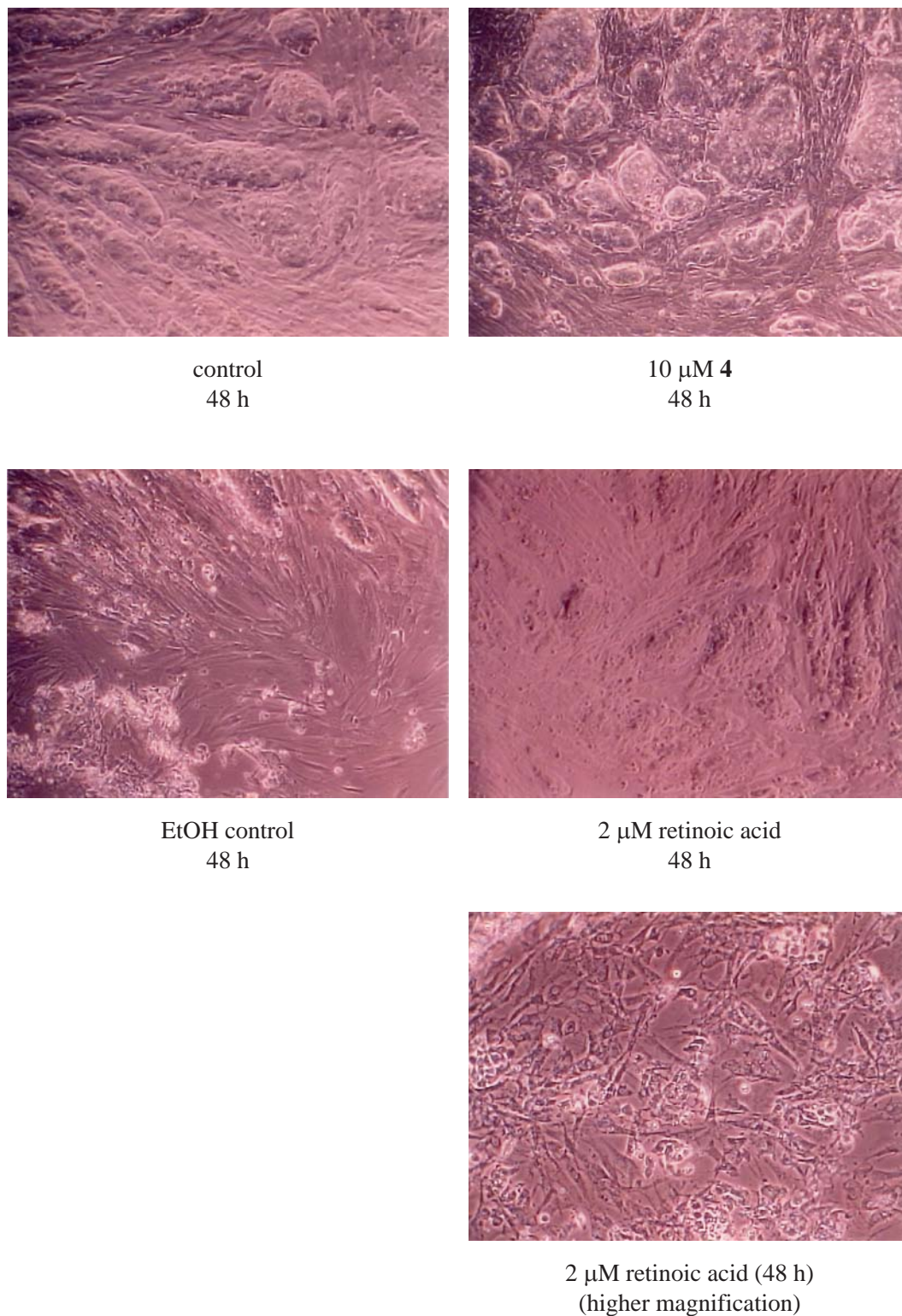


Figure 5.16. Images of R1 mouse embryonic stem cells after 48 h treatment. Untreated cell samples, as well as samples treated with 10 μM **4**, EtOH only, and 2 μM retinoic acid dosed in EtOH, are shown following 48 hours of incubation with the compound indicated. A higher magnification image of retinoic acid-treated sample is shown at bottom.

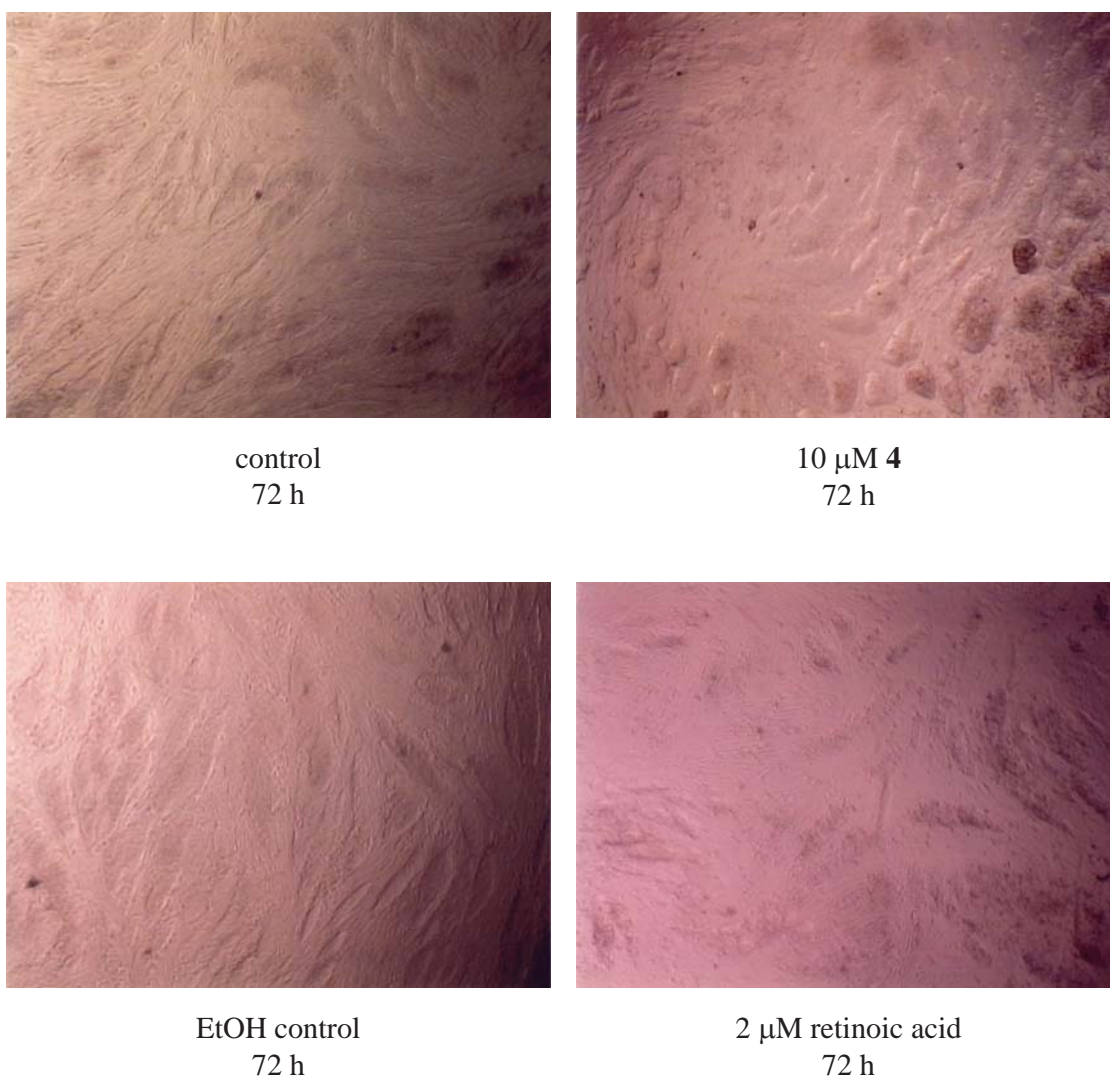


Figure 5.17. Images of R1 mouse embryonic stem cells after 72 h treatment. Untreated cell samples, as well as samples treated with 10 μM 4, EtOH only, and 2 μM retinoic acid dosed in EtOH, are shown following 72 hours of incubation with the compound indicated.

5.3. Conclusion and future directions

The gene expression levels of Oct4 target genes that contain an Oct4 transcription factor binding site in the enhancer region were assayed by quantitative RT-PCR. Based on melting temperature analysis of a series of polyamides designed to target the DNA sequence 5'-WTGCWW-3', polyamide **4**, which contains a free chiral amine on the 3,4-diaminobutyric turn linkage, exhibits the highest binding affinity. After 48 h incubation time with 5 μ M of polyamide **4** in a P19 mouse embryonal carcinoma cell line, Utf1 mRNA levels were decreased by 60%. However, it was surprising to observe that Sox2 mRNA levels were increased two-fold. After 72 h incubation time with 10 μ M of polyamide **4** in a R1 mouse embryonic stem cell line, Utf1 mRNA levels were decreased by 40%. In contrast, Sox2 mRNA levels only increased modestly, and Nanog mRNA levels were increased two-fold. The cell morphology of polyamide-treated samples appeared similar to untreated samples by visual inspection.

The treatment of R1 embryonic stem cells with 2 μ M retinoic acid chemically induces differentiation that was evident after 24 h and 48 h. While Utf1 downregulation and Nanog de-repression were comparable in the retinoic acid-treated and polyamide-treated samples, no changes in cell morphology were observed after incubation with polyamide **4** for 72 h. Polyamide-induced differentiation of mouse embryonic stem cells may require longer time-course experiments. However, the healthy growth of mouse embryonic stem cells when incubated with 10 μ M of polyamide **4** is an encouraging sign that higher concentrations may be tolerated in future experiments.

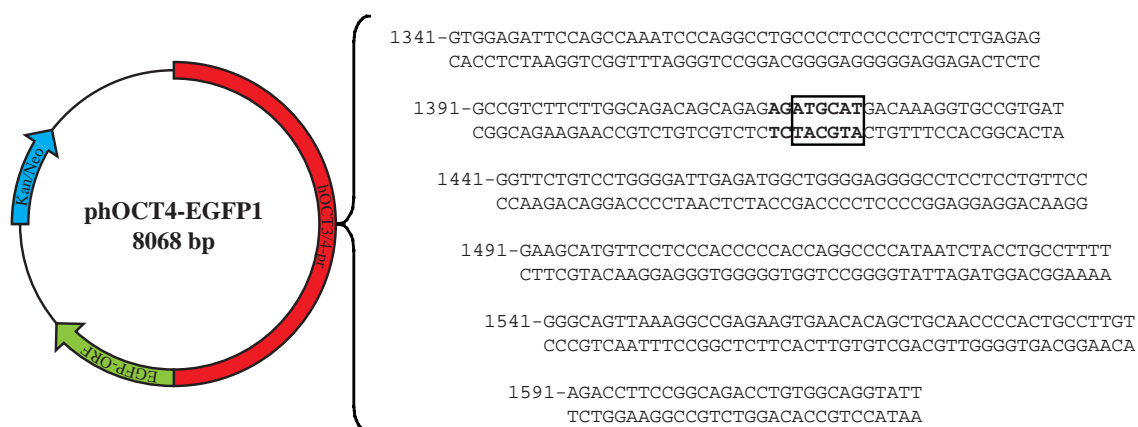


Figure 5.18. The partial sequence of plasmid phOCT4-EGFP1. The equilibrium association constant (K_a) of polyamide **1** was determined by DNase I footprint titration experiments on the Oct4 binding site of the phOCT4-EGFP1 plasmid obtained from Dr. Wei Cui of the Roslin Institute.³⁴

5.4. Materials and methods

5.4.1. Polyamide synthesis

Polyamides were synthesized with oxime resin (compounds **1-12**, Novabiochem) or Boc- β -Ala-PAM resin (compounds **13-14**, Peptides International) according to published manual solid-phase synthesis protocols.^{31,32} For compounds **1-3**, **6**, **8**, **10**, **13**, and **14**, *N*- α -9-fluorenylmethoxycarbonyl-*N*- γ -*tert*-butoxycarbonyl-D-2,4-diaminobutyric acid (Fmoc-D-Dab(Boc)-OH, Peptides International) was used for the turn linkage. The protected ^{FmocHN} γ -turn amine was deprotected with 20% piperidine in DMF and reprotected as the Boc derivative with a solution of Boc₂O (Fluka) and DIEA in DMF. For compounds **1** and **3**, the protected ^{BocHN} γ -turn amine was deprotected with 20% trifluoroacetic acid (TFA, Halocarbon) in DCM and reprotected as the acetylated derivative with a solution of acetic anhydride and DIEA in NMP. For compounds **2**, **6**, **8**, **10**, **13**, and **14**, the Boc-protected amine was left untreated. For compounds **4**, **5**, **7**, **9**, **11**, and **12**, *N*- β -benzyloxycarbonyl-*N*- γ -*tert*-butoxycarbonyl-R-3,4-diaminobutyric acid (Z-Dbu(Boc)-OH, Senn Chemicals AG) was used for the turn linkage. For compounds **1-5**, the chlorothiophene-imidazole cap was added on solid phase as a dimer.

The acetylated or Boc-protected or Cbz-protected resin was cleaved with 1 mL of 3,3'-diamino-*N*-methyldipropylamine at 37°C with agitation for 16 h. Products were purified by preparatory reverse-phase high-performance liquid chromatography (HPLC) on a Beckman Gold system using a Phenomenex Gemini 21.2 mm \times 250 mm, 5 μ m 110 Å C₁₈ reverse-phase column in 0.1% (w/v) TFA with acetonitrile as the eluent. The appropriate fractions were lyophilized after characterization by analytical HPLC, UV-visible spectroscopy, and matrix-assisted laser desorption ionization/time-of-flight mass spectrometry (MALDI-TOF-MS). HPLC analysis was performed on a Beckman Gold system equipped with a diode-array detector using a Phenomenex Gemini 4.6 mm \times 250 mm, 5 μ m 110 Å C₁₈ reverse-phase column. UV spectra were measured on an Agilent Technologies 8453 UV-vis ChemStation spectrophotometer. MALDI-TOF-MS was carried

out on an Applied Biosystems Voyager DE-PRO.

FITC conjugate **1** was formed by reacting fluorescein-5-isothiocyanate (Invitrogen) with the acetylated polyamide in a solution of DIEA (20 equiv) and DMF for 1 h at room temperature. The product was purified by preparatory reverse-phase HPLC, and lyophilization of the appropriate fractions yielded the polyamide-fluorescein conjugate **1**, which was characterized as described above.

IPA conjugates **2-14** were formed by pre-activating isophthalic acid (IPA, 3.0 equiv) with PyBOP (2.9 equiv, Novabiochem) in a solution of DIEA (20 equiv) and DMF at 37°C for 30 min, followed by reaction of the activated solution with the polyamide for 1 h at room temperature. For conjugate **3**, the product was purified by preparatory reverse-phase HPLC, and lyophilization of the appropriate fractions yielded the acetylated IPA conjugate **3**. For conjugates **2, 6, 8, 10, 13**, and **14**, conjugates were deprotected with neat TFA and triethylsilane for 30 min at room temperature before purification.

For conjugates **4, 7, 9, 11**, and **12**, the product was purified by solid-phase extraction using a Waters SepPak C-18 Light Cartridge following conjugation with isophthalic acid. The eluted fractions in acetonitrile and methanol were lyophilized. The Cbz protecting group was removed according to published protocols.²⁸ A 500 nmol fraction of the Cbz-protected hairpin polyamide conjugate was dissolved in 450 μ L TFA and 50 μ L trifluoromethanesulfonic acid (TFMSA). After a reaction time of 5 min, the solution was flash frozen in liquid nitrogen and overlaid with 1 mL DMF. The thawed solution was diluted in 20% aqueous acetonitrile for purification by preparatory reverse-phase HPLC. Lyophilization of the appropriate fractions yielded the IPA conjugates **4, 7, 9, 11**, and **12**.

Conjugate **5** was synthesized by acetylation of conjugate **4**, according to published protocols.²⁸ Polyamide conjugate **4** was dissolved in 1200 μ L DMF. A mixture of 135 μ L pyridine and 15 μ L acetic anhydride was added, and the reaction was allowed to proceed for 30 min at room temperature. The product was purified by preparatory reverse-phase HPLC, and lyophilization of the appropriate fractions yielded the acetylated IPA conjugate

5. For conjugates **1-14**, extinction coefficients were calculated according to standard protocols.³⁷ Chemicals not otherwise specified were from Aldrich.

CtImPyPy-(R)^{AcHN} γ -PyImPyPy-(+)-FITC (1). Synthesized with 2,4-diaminobutyric acid turn subunit and conjugated with fluorescein-5-isothiocyanate (FITC). UV-vis $\lambda_{\text{max}} = 307, 444$ nm; MALDI-TOF-MS m/z 1288.94 ($\text{C}_{58}\text{H}_{71}\text{ClN}_{21}\text{O}_{10}\text{S}^+$ calculated [M+H-FITC]⁺ 1288.51)

CtImPyPy-(R)^{H₂N} γ -PyImPyPy-(+)-IPA (2). Synthesized with 2,4-diaminobutyric acid turn subunit and conjugated with isophthalic acid (IPA). UV-vis $\lambda_{\text{max}} = 318$ nm; MALDI-TOF-MS m/z 1394.86 ($\text{C}_{64}\text{H}_{73}\text{ClN}_{21}\text{O}_{12}\text{S}^+$ calculated [M+H]⁺ 1394.52)

CtImPyPy-(R)^{AcHN} γ -PyImPyPy-(+)-IPA (3). Synthesized with 2,4-diaminobutyric acid turn subunit and conjugated with isophthalic acid (IPA). UV-vis $\lambda_{\text{max}} = 314$ nm; MALDI-TOF-MS m/z 1436.74 ($\text{C}_{66}\text{H}_{75}\text{ClN}_{21}\text{O}_{13}\text{S}^+$ calculated [M+H]⁺ 1436.53)

CtImPyPy-(R)^{H₂N} γ -PyImPyPy-(+)-IPA (4). Synthesized with 3,4-diaminobutyric acid turn subunit and conjugated with isophthalic acid (IPA). UV-vis $\lambda_{\text{max}} = 318$ nm; MALDI-TOF-MS m/z 1394.76 ($\text{C}_{64}\text{H}_{73}\text{ClN}_{21}\text{O}_{12}\text{S}^+$ calculated [M+H]⁺ 1394.52)

CtImPyPy-(R)^{AcHN} γ -PyImPyPy-(+)-IPA (5). Synthesized with 3,4-diaminobutyric acid turn subunit and conjugated with isophthalic acid (IPA). UV-vis $\lambda_{\text{max}} = 314$ nm; MALDI-TOF-MS m/z 1436.78 ($\text{C}_{66}\text{H}_{75}\text{ClN}_{21}\text{O}_{13}\text{S}^+$ calculated [M+H]⁺ 1436.53)

The synthesis and characterization of polyamide conjugates **6-14** have been reported previously.^{33,35}

5.4.2. Quantitative DNase I footprint titrations

Quantitative DNase I footprint titration experiments were performed on the 5'-³²P-end-labeled PCR products of plasmid phOCT4-EGFP1 according to standard protocols.³⁷ The phOCT4-EGFP1 plasmid was a gift from Dr. Wei Cui of the Roslin Institute.³⁴ Radiolabeled DNA was equilibrated with a solution of polyamide **1** for 14-16 h at 22°C in a buffer of 10 mM Tris-HCl, 10 mM KCl, 10 mM MgCl₂, and 5 mM CaCl₂ at pH 7.0

prior to DNase I cleavage. Chemical sequencing reactions were performed according to published methods.^{38,39} Storage phosphor autoradiography was performed on a Molecular Dynamics Typhoon 8600 phosphorimager. 18 M Ω water was obtained from an AquaMAX Ultra water purification system, and all buffers were 0.2 μ m filtered.

5.4.3. UV absorption spectrophotometry

Melting temperature analysis was performed according to published protocols.²⁸ UV absorption analysis was performed on a Varian Cary 100 spectrophotometer. Analysis was performed in a degassed aqueous buffer of 10 mM sodium cacodylate, 10 mM KCl, 10 mM MgCl₂, and 5 mM CaCl₂ at pH 7.0. The 12 bp DNA oligonucleotides 5'-GAGATGCATGAC-3' and 5'-GTCATGCATCTC-3' were obtained with HPLC purification from Integrated DNA Technologies. The DNA oligonucleotides and polyamides **1-5** were mixed in 1:1 stoichiometry to a final concentration of 2 μ M in a volume of 1 mL for each experiment. Prior to analysis, samples were heated to 90°C and cooled to a starting temperature of 25°C with a heating or cooling rate of 5°C/min for each ramp. Denaturation profiles were recorded at λ = 260 nm from 25°C to 90°C with a heating rate of 0.5°C/min. The reported melting temperatures were defined as the maximum of the first derivative of the denaturation profile.

5.4.4. Cell cultures

Cell lines were cultured in a 5% CO₂ atmosphere at 37°C. The human cervical cancer cell line HeLa and the mouse embryonal carcinoma cell line P19 were obtained from ATCC and cultured according to recommended protocols. HeLa cells were cultured in DMEM medium (Invitrogen) supplemented with 10% fetal bovine serum (FBS, Omega Scientific) and 1% penicillin/streptomycin solution (Mediatech).^{29,30} P19 cells were cultured in Alpha Minimum Essential Medium with ribonucleosides and deoxyribonucleosides (Invitrogen) supplemented with 7.5% bovine calf serum (Omega Scientific) and 2.5% fetal bovine

serum. R1 mouse embryonic stem cells were cultured according to standard protocols by Caltech Genetically Engineered Mouse Services. The R1 mouse embryonic stem cell line was obtained from the Nagy lab, where they were developed.

5.4.5. Confocal microscopy

Confocal microscopy experiments were performed according to published protocols.^{29,30} Cell lines were trypsinized (Mediatech) for 5 min at 37°C, centrifuged for 10 min at 4°C at 100 × g, and resuspended in fresh medium to a concentration of 1.33×10^5 cells/mL. Incubations were performed by adding 150 µL of cells into culture dishes equipped with glass bottoms for direct imaging (MatTek). Cells were grown in the glass-bottom culture dishes for 24 h. The medium was then removed and replaced with 147 µL of fresh medium, followed by addition of 3 µL of the 100 µM solution of polyamide-fluorescein conjugate **1** for a final polyamide concentration of 2 µM. Cells were incubated in a 5% CO₂ atmosphere at 37°C for 12 h. Imaging was performed with a 63× oil-immersion objective lens on a Zeiss LSM 5 Pascal inverted laser scanning microscope. Polyamide-fluorescein conjugate fluorescence and visible light images were obtained using standard filter sets for fluorescein.^{29,30}

5.4.6. Quantitative RT-PCR experiments

For cell culture experiments, P19 mouse embryonal carcinoma cells were plated in a 24-well format with a concentration of 5×10^4 cells/mL in a volume of 500 µL. Polyamides were added to the medium at this time as a solution in water. RNA was harvested after 48 h incubation using an RNeasy Mini Kit (Qiagen) and reverse transcribed using SuperScript II Reverse Transcriptase (Invitrogen). Quantitative RT-PCR was performed using SYBR GREEN PCR Master Mix (Applied Biosystems) on an Applied Biosystems 7300 Real Time PCR System. Gene expression levels were measured relative to Gapdh.

R1 mouse embryonic stem cells were cultured according to standard protocols by Caltech Genetically Engineered Mouse Services. The R1 mouse embryonic stem cell line was obtained from the Nagy lab, where they were developed. R1 mouse embryonic stem cells were plated in a 24-well format on a feeder layer of mouse primary fibroblasts. Polyamides were added to the medium as a solution in water. Cocktail 1 contains 5 μ M each of polyamides **6**, **8**, **9**, and **10**. Cocktail 2 contains 5 μ M each of polyamides **11-14**. Retinoic acid (Fluka) was added to the medium as a solution in ethanol. As a control, an equivalent volume of ethanol without retinoic acid was added to the medium. RNA was harvested after 48 h or 72 h using the same procedure described above.

Stealth RNAi transfection experiments were performed according to recommended protocols for P19 cells from Invitrogen. For Oct4 (Pou5f1) Stealth RNAi experiments, P19 cells were plated in a 24-well format with a concentration of 1×10^5 cells/mL in a volume of 400 μ L growth medium without antibiotics one day before transfection. For each transfection sample, 50 pmol of Stealth RNAi was diluted in 50 μ L of Opti-MEM I Reduced Serum Medium. Separately, 1 μ L of Lipofectamine 2000 was diluted in 50 μ L of Opti-MEM I Reduced Serum Medium and incubated for 15 min at room temperature. The diluted Stealth RNAi and Lipofectamine 2000 solutions were combined and incubated for 15 min at room temperature before addition to each well.

Stealth RNAi for the Pou5f1 gene was obtained from Invitrogen. Duplex #1 contained the 25 bp RNA oligonucleotides 5'-CCAAUGCCGUGAAGUUGGAGAAGGU-3' and 5'-ACCUUCUCCAACUUCACGGCAUUGG-3'. Duplex #2 contained the 25 bp RNA oligonucleotides 5'-CCCGGAAGAGAAAGCGAACUAGCAU-3' and 5'-AUGCUAGUUCGCUUUCUCUUCGCGG-3'. Duplex #3 contained the 25 bp RNA oligonucleotides 5'-CCAAUCAGCUUGGGCUAGAGAAGGA-3' and 5'-UCCUUCUCUAGCCCAAGCUGAUUGG-3'. While all three Stealth RNAi duplexes

achieved knockdown of the gene of interest, duplex #2 was the most effective. A negative Stealth RNAi containing medium GC content (Invitrogen, Lot #434330) was used as a control.

5.4.7. Primers for quantitative RT-PCR

The following sets of primers were used for quantitative RT-PCR experiments. Oligonucleotides were obtained from Integrated DNA Technologies in LabReady format normalized to 100 μ M in IDTE pH 8.0. PCR amplicons were analyzed by gel electrophoresis on a 2% agarose gel (Invitrogen) stained with SYBR Gold (Invitrogen) and imaged on a Molecular Dynamics Typhoon 8600. PCR amplification efficiency and dissociation curve analysis were performed as recommended by Applied Biosystems.

Gapdh_03_L: 5'-CGTCCCGTAGACAAAATGGT-3' (20 bp, 36-55)

Gapdh_03_R: 5'-TTGATGGCAACAATCTCCAC-3' (20 bp, 126-145)

110 bp amplicon

Pou5f1_02_L: 5'-GTTGGAGAAGGTGGAACCAA-3' (20 bp, 415-434)

Pou5f1_02_R: 5'-TCTTCTGCTTCAGCAGCTTG-3' (20 bp, 490-509)

95 bp amplicon

Sox2_01_L: 5'-GCACATGAACGGCTGGAGCAACG-3' (23 bp, 900-922)

Sox2_01_R: 5'-TGCTGCGAGTAGGACATGCTGTAGG-3' (25 bp, 1082-1106)

207 bp amplicon

Nanog_01_L: 5'-TCTTCCTGGTCCCCACAGTTT-3' (21 bp, 227-247)

Nanog_01_R: 5'-GCAAGAATAGTTCTCGGGATGAA-3' (23 bp, 304-326)

100 bp amplicon

Utf1_01_L: 5'-GTCCCTCTCCGCGTTAGC-3' (18 bp, 531-548)

Utf1_01_R: 5'-GGAAGAAGTGAATCTGAGCG-3' (20 bp, 620-639)

109 bp amplicon

Utf1_02_L: 5'-TGTCCCGGTGACTACGTCT-3' (19 bp, 102-120)

Utf1_02_R: 5'-CCCAGAAGTAGCTCCGTCTCT-3' (21 bp, 216-236)

135 bp amplicon

Fbx15_01_L: 5'-TGCCAATTGTTGGGAGTACA-3' (20 bp, 111-130)

Fbx15_01_R: 5'-CATGCTGCTTCGTGACAGAT-3' (20 bp, 184-203)

93 bp amplicon

Fbx15_04_L: 5'-TGTTAGAGGCTCATCTGTCACG-3' (22 bp, 172-193)

Fbx15_04_R: 5'-GATGGCATTCTGTCCAGGGAT-3' (21 bp, 256-276)

105 bp amplicon

Fgf4_02_L: 5'-GTGTGCCTTTCTTTACCGACG-3' (21 bp, 547-567)

Fgf4_02_R: 5'-CTGAGGGCCATGAACATACCG-3' (21 bp, 632-652)

106 bp amplicon

Acknowledgments.

We thank Shirley Pease and the Caltech Genetically Engineered Mouse Services for assistance with R1 mouse embryonic stem cell experiments. We are grateful to the National Institutes of Health for research support.

John Phillips performed quantitative DNase I footprint titration experiments. Daniel Harki synthesized polyamides **6**, **7**, and **9-14**. James Puckett synthesized polyamides **7** and **8**.

References

1. Wobus, A.M. and Boheler, K.R. (2005) Embryonic stem cells: Prospects for developmental biology and cell therapy. *Physiol. Rev.*, **85**, 635-678.
2. Chambers, I. and Smith, A. (2004) Self-renewal of teratocarcinoma and embryonic stem cells. *Oncogene*, **23**, 7150-7160.
3. Rodda, D.J., Chew, J.L., Lim, L.H., Loh, Y.H., Wang, B., Ng, H.H. and Robson, P. (2005) Transcriptional regulation of Nanog by Oct4 and Sox2. *J. Biol. Chem.*, **280**, 24731-24737.
4. Pesce, M., Gross, M.K. and Scholer, H.R. (1998) In line with our ancestors: Oct-4 and the mammalian germ. *Bioessays*, **20**, 722-732.
5. Pesce, M. and Scholer, H.R. (2001) Oct-4: Gatekeeper in the beginnings of mammalian development. *Stem Cells*, **19**, 271-278.
6. Pan, G.J., Chang, Z.Y., Scholer, H.R. and Pei, D.Q. (2002) Stem cell pluripotency and transcription factor Oct4. *Cell Res.*, **12**, 321-329.
7. Niwa, H., Miyazaki, J. and Smith, A.G. (2000) Quantitative expression of Oct-3/4 defines differentiation, dedifferentiation or self-renewal of ES cells. *Nature Genet.*, **24**, 372-376.
8. Takahashi, K. and Yamanaka, S. (2006) Induction of pluripotent stem cells from mouse embryonic and adult fibroblast cultures by defined factors. *Cell*, **126**, 663-

676.

9. Takahashi, K., Tanabe, K., Ohnuki, M., Narita, M., Ichisaka, T., Tomoda, K. and Yamanaka, S. (2007) Induction of pluripotent stem cells from adult human fibroblasts by defined factors. *Cell*, **131**, 861-872.

10. Yu, J.Y., Vodyanik, M.A., Smuga-Otto, K., Antosiewicz-Bourget, J., Frane, J.L., Tian, S., Nie, J., Jonsdottir, G.A., Ruotti, V., Stewart, R., Slukvin, II and Thomson, J.A. (2007) Induced pluripotent stem cell lines derived from human somatic cells. *Science*, **318**, 1917-1920.

11. Lewitzky, M. and Yamanaka, S. (2007) Reprogramming somatic cells towards pluripotency by defined factors. *Curr. Opin. Biotechnol.*, **18**, 467-473.

12. Niwa, H. (2007) How is pluripotency determined and maintained? *Development*, **134**, 635-646.

13. Herr, W. and Cleary, M.A. (1995) The Pou Domain - Versatility in Transcriptional Regulation by a Flexible 2-in-One DNA-Binding Domain. *Genes Dev.*, **9**, 1679-1693.

14. Chew, J.L., Loh, Y.H., Zhang, W.S., Chen, X., Tam, W.L., Yeap, L.S., Li, P., Ang, Y.S., Lim, B., Robson, P. and Ng, H.H. (2005) Reciprocal transcriptional regulation of Pou5f1 and Sox2 via the Oct4/Sox2 complex in embryonic stem cells. *Mol. Cell. Biol.*, **25**, 6031-6046.

15. Remenyi, A., Lins, K., Nissen, L.J., Reinbold, R., Scholer, H.R. and Wilmanns, M.

- (2003) Crystal structure of a POU/HMG/DNA ternary complex suggests differential assembly of Oct4 and Sox2 on two enhancers. *Genes Dev.*, **17**, 2048-2059.
16. Tomioka, M., Nishimoto, M., Miyagi, S., Katayanagi, T., Fukui, N., Niwa, H., Muramatsu, M. and Okuda, A. (2002) Identification of Sox-2 regulatory region which is under the control of Oct-3/4-Sox-2 complex. *Nucleic Acids Res.*, **30**, 3202-3213.
 17. Masui, S., Nakatake, Y., Toyooka, Y., Shimosato, D., Yagi, R., Takahashi, K., Okochi, H., Okuda, A., Matoba, R., Sharov, A.A., Ko, M.S.H. and Niwa, H. (2007) Pluripotency governed by Sox2 via regulation of Oct3/4 expression in mouse embryonic stem cells. *Nat. Cell Biol.*, **9**, 625-U26.
 18. Boer, B., Kopp, J., Mallanna, S., Desler, M., Chakravarthy, H., Wilder, P.J., Bernadt, C. and Rizzino, A. (2007) Elevating the levels of Sox2 in embryonal carcinoma cells and embryonic stem cells inhibits the expression of Sox2 : Oct-3/4 target genes. *Nucleic Acids Res.*, **35**, 1773-1786.
 19. Pan, G.J. and Thomson, J.A. (2007) Nanog and transcriptional networks in embryonic stem cell pluripotency. *Cell Res.*, **17**, 42-49.
 20. Loh, Y.H., Wu, Q., Chew, J.L., Vega, V.B., Zhang, W.W., Chen, X., Bourque, G., George, J., Leong, B., Liu, J., Wong, K.Y., Sung, K.W., Lee, C.W.H., Zhao, X.D., Chiu, K.P., Lipovich, L., Kuznetsov, V.A., Robson, P., Stanton, L.W., Wei, C.L., Ruan, Y.J., Lim, B. and Ng, H.H. (2006) The Oct4 and Nanog transcription network regulates pluripotency in mouse embryonic stem cells. *Nature Genet.*, **38**, 431-

440.

21. Nishimoto, M., Fukushima, A., Okuda, A. and Muramatsu, M. (1999) The gene for the embryonic stem cell coactivator UTF1 carries a regulatory element which selectively interacts with a complex composed of Oct-3/4 and Sox-2. *Mol. Cell. Biol.*, **19**, 5453-5465.
22. Tokuzawa, Y., Kaiho, E., Maruyama, M., Takahashi, K., Mitsui, K., Maeda, M., Niwa, H. and Yamanaka, S. (2003) Fbx15 is a novel target of Oct3/4 but is dispensable for embryonic stem cell self-renewal and mouse development. *Mol. Cell. Biol.*, **23**, 2699-2708.
23. Dailey, L., Yuan, H.B. and Basilico, C. (1994) Interaction between a Novel F9-Specific Factor and Octamer-Binding Proteins Is Required for Cell-Type-Restricted Activity of the Fibroblast Growth-Factor-4 Enhancer. *Mol. Cell. Biol.*, **14**, 7758-7769.
24. Dervan, P.B. (2001) Molecular recognition of DNA by small molecules. *Bioorg. Med. Chem.*, **9**, 2215-2235.
25. Dervan, P.B. and Edelson, B.S. (2003) Recognition of the DNA minor groove by pyrrole-imidazole polyamides. *Curr. Opin. Struct. Biol.*, **13**, 284-299.
26. Nickols, N.G., Jacobs, C.S., Farkas, M.E. and Dervan, P.B. (2007) Improved nuclear localization of DNA-binding polyamides. *Nucleic Acids Res.*, **35**, 363-370.
27. Herman, D.M., Baird, E.E. and Dervan, P.B. (1998) Stereochemical control of the

DNA binding affinity, sequence specificity, and orientation preference of chiral hairpin polyamides in the minor groove. *J. Am. Chem. Soc.*, **120**, 1382-1391.

28. Dose, C., Farkas, M.E., Chenoweth, D.M. and Dervan, P.B. (2008) Next generation hairpin polyamides with (R)-3,4-diaminobutyric acid turn unit. *J. Am. Chem. Soc.*, **130**, 6859-6866.
29. Best, T.P., Edelson, B.S., Nickols, N.G. and Dervan, P.B. (2003) Nuclear localization of pyrrole-imidazole polyamide-fluorescein conjugates in cell culture. *Proc. Natl. Acad. Sci. U. S. A.*, **100**, 12063-12068.
30. Edelson, B.S., Best, T.P., Olenyuk, B., Nickols, N.G., Doss, R.M., Foister, S., Heckel, A. and Dervan, P.B. (2004) Influence of structural variation on nuclear localization of DNA-binding polyamide-fluorophore conjugates. *Nucleic Acids Res.*, **32**, 2802-2818.
31. Baird, E.E. and Dervan, P.B. (1996) Solid phase synthesis of polyamides containing imidazole and pyrrole amino acids. *J. Am. Chem. Soc.*, **118**, 6141-6146.
32. Belitsky, J.M., Nguyen, D.H., Wurtz, N.R. and Dervan, P.B. (2002) Solid-phase synthesis of DNA binding polyamides on oxime resin. *Bioorg. Med. Chem.*, **10**, 2767-2774.
33. Nickols, N.G. and Dervan, P.B. (2007) Suppression of androgen receptor-mediated gene expression by a sequence-specific DNA-binding polyamide. *Proc. Natl. Acad.*

Sci. U. S. A., **104**, 10418-10423.

34. Gerrard, L., Zhao, D.B., Clark, A.J. and Cui, W. (2005) Stably transfected human embryonic stem cell clones express OCT4-specific green fluorescent protein and maintain self-renewal and pluripotency. *Stem Cells*, **23**, 124-133.
35. Olenyuk, B.Z., Zhang, G.J., Klco, J.M., Nickols, N.G., Kaelin, W.G. and Dervan, P.B. (2004) Inhibition of vascular endothelial growth factor with a sequence-specific hypoxia response element antagonist. *Proc. Natl. Acad. Sci. U. S. A.*, **101**, 16768-16773.
36. Kopp, J.L., Ormsbee, B.D., Desler, M. and Rizzino, A. (2008) Small increases in the level of Sox2 trigger the differentiation of mouse embryonic stem cells. *Stem Cells*, **26**, 903-911.
37. Trauger, J.W. and Dervan, P.B. (2001) Footprinting methods for analysis of pyrrole-imidazole polyamide/DNA complexes. *Methods in Enzymology*, **340**, 450-466.
38. Maxam, A.M. and Gilbert, W. (1980) Sequencing end-labeled DNA with base-specific chemical cleavages. *Methods in Enzymology*, **65**, 499-560.
39. Iverson, B.L. and Dervan, P.B. (1987) Adenine Specific DNA Chemical Sequencing Reaction. *Nucleic Acids Res.*, **15**, 7823-7830.